

# Novel Role of Superfluidity in Low-Energy Nuclear Reactions

Piotr Magierski<sup>1,2</sup>, Kazuyuki Sekizawa<sup>1</sup>, Gabriel Wlazłowski<sup>1,2</sup>

<sup>1</sup>*Faculty of Physics, Warsaw University of Technology,  
Ulica Koszykowa 75, 00-662 Warsaw, Poland and*

<sup>2</sup>*Department of Physics, University of Washington, Seattle, Washington 98195-1560, USA\**

We demonstrate, within symmetry unrestricted time-dependent density functional theory, the existence of new effects in low-energy nuclear reactions which originate from superfluidity. The dynamics of the pairing field induces solitonic excitations in the colliding nuclear systems, leading to qualitative changes in the reaction dynamics. The solitonic excitation prevents collective energy dissipation and effectively suppresses fusion cross section. We demonstrate how the variations of the total kinetic energy of the fragments can be traced back to the energy stored in the superfluid junction of colliding nuclei. Both contact time and scattering angle in non-central collisions are significantly affected. The modification of the fusion cross section and possibilities for its experimental detection are discussed.

PACS numbers: 25.70.-z, 25.70.Jj, 03.75.Lm, 74.40.Gh

*Introduction.*— Dynamics of the pairing field during the nuclear reactions has rarely been investigated to date, although it is well-known that the static pairing field is crucial for the description of the atomic nuclei, both in the ground state as well as in excited states (see, *e.g.*, [1–5] and references therein). The reason is twofold: first, it is believed that the pairing field dynamics will produce only small corrections to the commonly accepted picture of low-energy nuclear reactions; second, the proper treatment of the pairing field dynamics requires to use more advanced approaches resulting in rapid increase of computational complexity. On the other hand, it is well known that the pairing correlations give rise to abundant fascinating phenomena, like topological excitations, observed with great details in superfluid helium [6] or ultracold atomic gases [7, 8]. For example in experiments with ultracold atomic gases, where two clouds of atomic Bose-Einstein Condensates (BEC) are forced to merge, the interface between the two BECs may lose its superfluid character (solitonic excitation). This excitation is unstable and decays through quantum vortices [9, 10]. In this paper, we investigate the possibility of creating similar excitations in nuclear reactions, see Fig. 1.

The pairing field in nuclear systems is small in a sense that the ratio of its magnitude to the Fermi energy does not exceed 5%. It implies that BCS treatment is regarded as a justified approximation and the size of the Cooper pair is of the same order as the size of a heavy nucleus. Although the pairing field is small as compared to, *e.g.*, the unitary Fermi gas [11], it is important for the proper description of the nuclear systems: while it smears out shell effects responsible for static deformations, it also enables large-amplitude collective motion which otherwise would be strongly damped. Therefore the description of nuclear fission requires to take into account superfluidity as one of crucial ingredients [12–14]. Recently, it has been pointed out that dynamic excitations of the pairing field, which is absent in the static treatment, affect

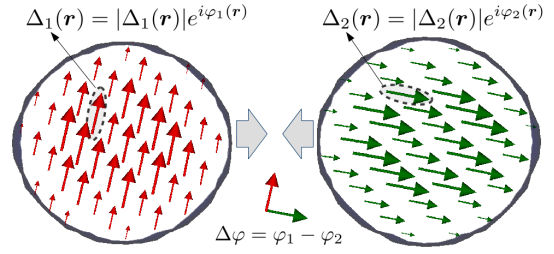


FIG. 1: (Color online) Schematic picture of the situation we examine in the present Letter: a collision of two superfluid nuclei with different phases of the pairing fields. Each disc represents a cross section of a nucleus. The arrows inside the nucleus indicate the pairing field  $\Delta_i(\mathbf{r})$  where length of the arrow indicates its absolute value  $|\Delta_i(\mathbf{r})|$ , while direction indicates its phase  $\varphi_i(\mathbf{r})$  ( $i = 1, 2$ ). In the ground state, the phase is uniform across each nucleus  $\varphi_i(\mathbf{r}) = \varphi_i$  and the phase difference  $\Delta\varphi$  ( $\equiv \varphi_1 - \varphi_2$ ) is well defined. We will show how the phase difference affects the reaction dynamics.

significantly the induced fission process leading to much longer fission timescales than predicted by other simplified approaches [15].

The pairing field  $\Delta(\mathbf{r})$  can be regarded as an order parameter that specifies whether the nucleus is superfluid or not [16]. The order parameter belongs to  $U(1)$  universality class and it can be decomposed as  $\Delta(\mathbf{r}) = |\Delta(\mathbf{r})|e^{i\varphi(\mathbf{r})}$ . In the ground state the phase is uniform across the nucleus, and it can be absorbed by the gauge transformation. Then the only relevant quantity is its absolute value  $|\Delta(\mathbf{r})|$  which is on the order of 1 MeV. The situation is different when two superfluid nuclei collide. Then the relative phase  $\Delta\varphi$  between two pairing fields is well defined (see Fig. 1) and cannot be removed by the gauge transformation. This difference will trigger various excitation modes of the pairing field as well as the particle flow between colliding nuclei. Although the phases of the pairing fields are not controlled in nuclear

experiments, they will affect the reaction outcomes in an averaged way. The consequences of this effect turn out to be significant and are discussed in this Letter.

*Collision of two superfluid nuclei.*— Let us first focus on the energy scale of the possible effect which may appear during a collision of two superfluid nuclei at a fixed pairing phase difference  $\Delta\varphi$ . One would naively expect that it is governed by the pairing energy which is proportional (for protons or neutrons) to  $\frac{1}{2}g(\varepsilon_F)|\Delta|^2$ , where  $g(\varepsilon_F)$  represents the density of states per one spin projection at the Fermi level, and  $\Delta$  is the pairing gap. Such quantity for nuclei is on the order of MeV, and thus one may infer that the possible effects would be too weak to be observed in nuclear reactions. However, this is not the case since during the collision a junction between two superfluids is created, where the phase varies rapidly. The energy stored in the junction depends both on the phase difference and the size of the junction. One may estimate the energy of the junction from phenomenological theory of superfluids, namely the Ginzburg-Landau (G-L) approach:

$$E_j = \frac{S}{L} \frac{\hbar^2}{2m} n_s \sin^2 \frac{\Delta\varphi}{2}, \quad (1)$$

where  $S$  is the area of the junction,  $L$  is the length scale over which the phase varies, and  $n_s$  is the superfluid density (for derivation, see [17]). Note that neither the pairing energy, nor the pairing gap enters this formula explicitly. For a collision of two heavy nuclei at energies close to the Coulomb barrier, one can show that the energy stored in the junction can vary by several tens of MeV depending on the phase difference [17]. Such a drastic energy change may significantly alter the dynamics of the collision. Clearly in order to determine those quantities in Eq. (1) ( $S, L, n_s$ ) one needs to perform microscopic simulations, since they are in general dependent on the actual reaction dynamics. Note that the situation described here is markedly different from the Josephson effect encountered in solids, ultra-cold atomic gases or heavy ion collisions [29–33]. The Josephson effect involves tunneling between weakly-coupled pairing condensates. Here we focus on the strong-coupling limit: the nature of the junction is entirely different even though its decay will also involve a Josephson-like current. In this Letter, we show that the associated pairing field dynamics has a significant impact on the fusion cross section and the total kinetic energy (TKE) of the fragments.

*TDSLDA for nuclear reactions.*— Presently, the most accurate microscopic approaches to the dynamics of superfluid systems are based on the density functional theory [34, 35]. Here we utilize an approximated formulation known as time-dependent superfluid local density approximation (TDSLDA), which is formally equivalent to the time-dependent Hartree-Fock-Bogoliubov theory (TDHFB). The approach has been proved to be very accurate for describing dynamics of strongly correlated

fermionic systems, like ultracold atomic gases [9, 10, 36–40] and nuclear systems [15, 41–43]. We solve the TDSLDA equations numerically on a 3D spatial lattice (without any symmetry restrictions) with periodic boundary conditions. We use a box of size 80 fm  $\times$  25 fm  $\times$  25 fm for head-on collisions and 80 fm  $\times$  60 fm  $\times$  25 fm for non-central collisions. The lattice spacing is set to 1.25 fm. For the energy density functional, we use FaNDF<sup>0</sup> functional [44, 45] without the spin-orbit term.

Although it is well known that the spin-orbit interaction is crucial for a proper description of nuclear static properties as well as energy dissipation in low-energy nuclear reactions, it does not induce qualitative change in the pairing field dynamics. In this Letter, we investigate possible impact of the phase difference on the reaction dynamics and address the following questions: what observables are affected by the phase difference and for each affected quantity what is the predicted size of the effect? In order to answer these questions one needs to set correctly the scales of the problem, which are determined in the present context by the average magnitude of the pairing gap and the ratio of the coherence length to the size of the system. None of the meaningful scales in our problem is affected by the spin-orbit interaction. However, in order to provide quantitative results that can be compared directly with experimental data, one needs to perform calculations with a full nuclear density functional. We defer these extremely numerically expensive studies to future works. This simplification allows us to construct a highly efficient solver of the TDSLDA equations (for details, see supplemental material of [18]). Nevertheless, the problem is still numerically demanding and requires usage of supercomputers. Very recently, the first attempt has been reported in [33], where the effects of the phase difference in head-on collisions of  $^{20}\text{O}+^{20}\text{O}$  were investigated based on TDHFB including the spin-orbit contribution. In case of reactions with light systems, the impact of the phase difference on various observables was found to be very small [33, 46].

One may rise a question regarding the adequacy of the description of the finite system using the theoretical framework admitting the broken particle-number symmetry. It gives rise to the Nambu-Goldstone (NG) modes related to the rotation of the phase of the pairing field [47, 48]. The phase can be traced back to the phase of the Cooper-pair wave function, which can be defined as the eigenfunction corresponding to the dominant eigenvalue of the two-body density matrix, and thus, is independent of a particular approximation in the treatment of the pairing correlations. The particle-number projected (symmetry-restored) wave function would imply averaging over the phase. The natural question is whether this averaging needs to be performed before the collision. The answer to this question is related to the timescale of the associated NG mode, which is governed by the nuclear chemical potentials [49]. Since phases of both projec-

tile and target nuclei rotate during the time evolution, what matters is the difference of the periods of the phase rotations. If it is long enough, as compared to the collision time, the use of the framework with broken particle-number symmetry is validated [50]. In the case of nuclear collision it is determined by the difference of (one nucleon) separation energies of the projectile and target nuclei  $\Delta S = |S_1 - S_2|$ . Thus, the description will be valid if one limits to the collision of nuclei whose difference between the separation energies does not exceed 1 MeV that leads  $T = \frac{2\pi\hbar}{\Delta S} > 1200 \text{ fm}/c$  which is longer than the collision time. The most clean case corresponds to the symmetric collision where the phase difference does not depend on time.

*Kinetic energy and Josephson current.*— As a first example, let us consider symmetric collisions of two heavy nuclei,  $^{240}\text{Pu}$  (since the spin-orbit term is neglected the nucleus does not exhibit a prolate deformation). In such a case two nuclei do not fuse and re-separate shortly after collision. In Fig. 2, we show pairing fields and densities of the colliding nuclei at various times in two extreme cases,  $\Delta\varphi = 0$  and  $\Delta\varphi = \pi$ . It is clearly visible that in the  $\Delta\varphi = \pi$  case a narrow solitonic structure is created, *i.e.* inside the structure the order parameter vanishes, the density is suppressed and the phase changes rapidly from one value to another when one crosses the structure. It stays there until the composite system splits. This produces a significant impact on resulting TKE of the fragments. In Fig. 3 (a), we show the TKE as a function of the relative phase for various collision energies. The TKE clearly shows the  $\sin^2 \frac{\Delta\varphi}{2}$  pattern (gray solid curves), which exactly recovers the dependence of the energy of the junction given by the G-L approach, Eq. (1). The dominating contribution comes from the neutron pairing field. The contribution from the proton pairing field is less than 30% of the neutron effect, due to Coulomb repulsion [17]. These results indicate that the phase difference hinders the energy transfer from the relative motion to internal degrees of freedom. We emphasize that the observed change of TKE cannot be attributed to the Josephson effect. For example, for extreme cases  $\Delta\varphi = 0$  and  $\Delta\varphi = \pi$ , there is no Josephson current (as it scales like  $\sin \Delta\varphi$ ) while dynamics of the reaction is altered.

The situation becomes qualitatively different when the energy is further increased. Namely, at energies about 30% above the barrier, the departure from this simple pattern is observed. It corresponds to the energies at which a third light fragment is generated [17]. The appearance of the third light fragment in the quasifission process is understood as a consequence of the density and charge excesses in the neck region [24]. However the solitonic excitation effectively reduces the density in the neck region. Consequently, for the energy range  $1.3V_{\text{Bass}} < E < 1.5V_{\text{Bass}}$  the number of fragments depends on the phase difference and smaller phase differ-

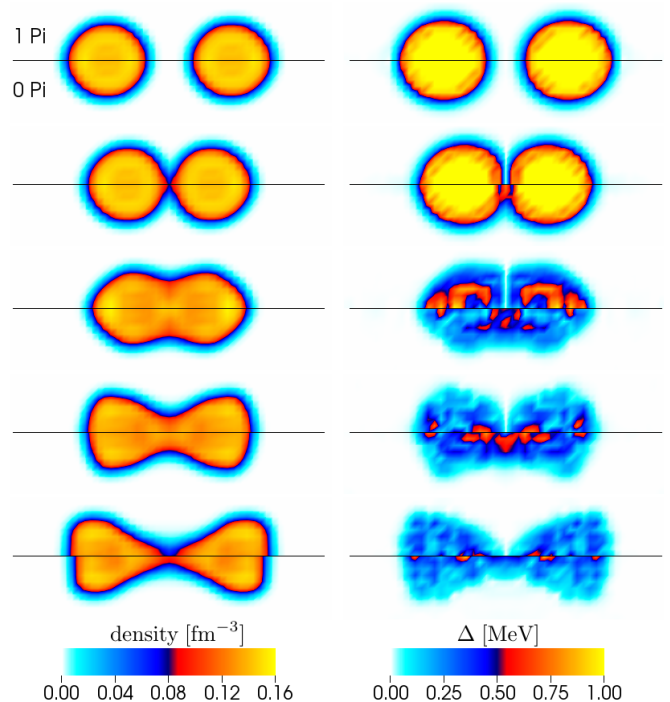


FIG. 2: (Color online) Snapshots from the collision of  $^{240}\text{Pu} + ^{240}\text{Pu}$  for two extreme values of the relative phase differences ( $\Delta\varphi = 0$  and  $\pi$ ) at the energy  $E \simeq 1.1V_{\text{Bass}}$ , where  $V_{\text{Bass}}$  represents the phenomenological fusion barrier [23]. Left panels show the total density distribution, whereas the right panels show the neutron pairing field of two colliding nuclei. Top half of each panel corresponds to the phase difference  $\Delta\varphi = \pi$  case, while bottom half corresponds to the case without phase difference  $\Delta\varphi = 0$ . Contact time is about 550–600 fm/c depending on the phase difference. For movies and plots showing the phase evolution see [17].

ences favour the creation of the third fragment [17]. For  $E > 1.5V_{\text{Bass}}$  the ternary quasifission is observed for all phase differences.

The stability of the solitonic excitation described here depends on the possibility of phase transfer between the pairing fields of the colliding nuclei, which manifests itself as particle transfer. Even though the reaction is symmetric, it can cause nucleon transfer from one nucleus to the other. Indeed, after re-separation the fragments are not symmetric. However, the amount of nucleon transfer does not exceed 1.5 for neutrons and 0.5 for protons during the collision (see, Fig. 3 (b) and [17] for more details). This result is consistent with earlier studies [29–33]. Note that this particle transfer resembles a Josephson current, even though the solitonic excitation itself has an entirely different origin.

*Energy threshold for fusion.*— Results for the heavy system indicate that the phase difference effectively works as a potential barrier, and consequently it will affect the fusion cross section. In order to investigate this issue, we examine collisions of two medium mass nuclei,

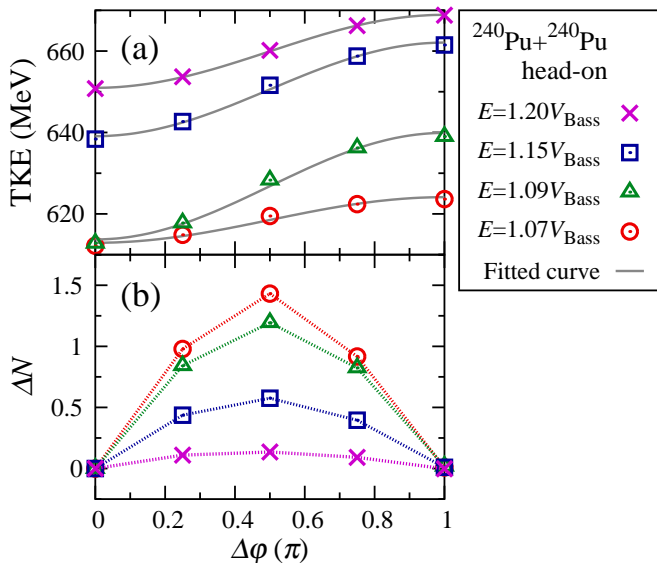


FIG. 3: (Color online) Results of the TDSLDA simulations for  $^{240}\text{Pu}+^{240}\text{Pu}$  head-on collisions at various collision energies. (a): Total kinetic energy (TKE) of the outgoing fragments is shown. Line shows fit to the data by a formula  $\alpha + \beta \sin^2 \frac{\Delta\varphi}{2}$  with respect to parameters  $\alpha$  and  $\beta$ . (b): The average number of transferred neutrons from the left nucleus to the right nucleus due to the Josephson current is shown. The horizontal axis is the relative pairing phase  $\Delta\varphi$ . Note that change of TKE has different phase dependence, and cannot be explained by the Josephson effect.

$^{90}\text{Zr}$ , that can fuse. Note that when the spin-orbit term is dropped this is an open-shell nucleus for neutrons and thus neutrons are superfluid, whereas protons occupy a closed shell. In Fig. 4, we show the minimum energy required for the system to merge in head-on collisions and stay in contact for times longer than 12000 fm/c (40 zs). The results clearly demonstrate that fusion reaction is effectively hindered by the dynamic excitations of the pairing field. The energy threshold as a function of the angle does not have  $\sin^2 \frac{\Delta\varphi}{2}$  dependence, since we consider now collisions varying both the phase difference and the collision energy.

The fusion hindrance phenomenon associated with pairing dynamics may likely be observed by studies of the fusion cross section for symmetric systems at the vicinity of the barrier, in a similar way to experimental detection of the so-called extra-push energy [51, 52], which is the energy introduced by Swiatecki to explain the experimental fusion cross sections for collisions of medium and heavy nuclei at energies above the Coulomb barrier [53–55]. As a good candidate we suggest symmetric collisions of different Zr isotopes. For these reactions the extra-push energy is negligible.  $^{90}\text{Zr}$  is neutron magic ( $N = 50$ ) and the pairing correlations are absent. As the neutron number increases neutrons become superfluid which hinders the fusion reaction. Based on our re-

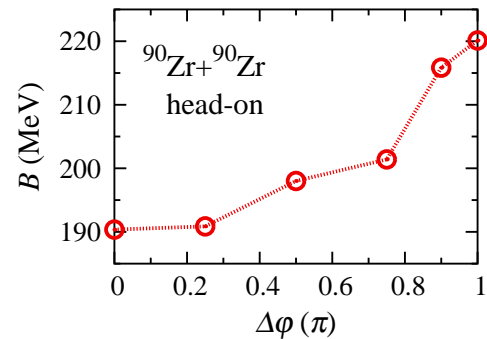


FIG. 4: (Color online) Results of the TDSLDA simulations for  $^{90}\text{Zr}+^{90}\text{Zr}$  head-on collisions. Fusion threshold energy  $B$  is shown as a function of the relative pairing phase  $\Delta\varphi$ . For this reaction the barrier height is  $V_{\text{Bass}} \simeq 192$  MeV. The phase difference prevents fusion for energies up to 15% above the barrier.

sults the extra energy for fusion is expected to be about  $E_{\text{extra}} = \frac{1}{\pi} \int_0^\pi (B(\Delta\varphi) - V_{\text{Bass}}) d(\Delta\varphi) \approx 10$  MeV.

Another possibility is to investigate asymmetric reactions like  $^{90-96}\text{Zr}+^{124}\text{Sn}$ . Despite the fact that the extra-push model predicts that the extra-push energy becomes smaller with increasing the neutron excess, the experimental data suggest the opposite trend [51]. TDHF calculations also show similar disagreement [56]. The measured trend is consistent with the results presented here, as the fusion reaction is hindered as the system departs from the neutron magic  $^{90}\text{Zr}$ . The chemical potentials for colliding nuclei are fairly similar admitting the description within broken particle-number symmetry. We have performed exploratory simulations for asymmetric reactions, and we have found that, similarly to the symmetric case, the phase difference can hinder the fusion for energies around the barrier, however no clear solitonic structure was observed [17].

Finally, we have also performed simulations of non-central collisions. If we are in the energy window where the phase difference can hinder the fusion, we find that it affects the contact time, and consequently the scattering angle is affected (see [17] for movies demonstrating this effect).

*Summary.*— We have investigated collisions of medium and heavy nuclei at energies around the Coulomb barrier taking into account the pairing field dynamics with TDFT for superfluid systems. We have found that during collision a stable soliton-like structure appears when two superfluid nuclei collide with phase difference of the pairing fields close to  $\Delta\varphi = \pi$ . The solitonic excitation suppresses the neck formation and hinders energy dissipation as well as fusion reaction, leading to significant changes in reaction dynamics. It implies that the pairing field dynamics effectively increases the barrier height for fusion resembling “thud wall” in the extra-push model, although at much smaller energies. The Josephson cur-

rent between two colliding nuclei turns out to be small, does not exceed 2 particles. The effects on the kinetic energy of the fragments and fusion cross section may likely be observed experimentally. Last but not least, it is to be reminded that the effects studied in this Letter are clearly beyond the commonly used TDHF+BCS approach [27, 28, 57–59] (see [17] for a detailed discussion).

We are in particular grateful to George Bertsch and Aurel Bulgac for discussions and critical remarks. We would like also to thank Nicholas Keeley, Michal Kowal, Eryk Piasecki, Krzysztof Rusek, Janusz Skalski for helpful discussions. We thank Witold Rudnicki, Franciszek Rakowski, Maciej Marchwiany and Kajetan Dutka from the Interdisciplinary Centre for Mathematical and Computational Modelling (ICM) of Warsaw University for useful discussions concerning the code optimization. This work was supported by the Polish National Science Center (NCN) under Contracts No. UMO-2013/08/A/ST3/00708. The code used for generation of initial states was developed under grant of Polish NCN under Contracts No. UMO-2014/13/D/ST3/01940. Calculations have been performed at HA-PACS (PACS-VIII) system—resources provided by Interdisciplinary Computational Science Program in Center for Computational Sciences, University of Tsukuba. The contribution of each one of the authors has been significant and the order of the names is alphabetical.

*Note added.*— Recently, in a related work [60], it has been shown that the phase difference can influence the outcome of the collision only in the case of systems characterized by the weak pairing correlations (like systems discussed here). In the strong pairing limit, the role of the initial phase difference is erased.

---

\* Electronic address: magiersk@if.pw.edu.pl, sekizawa@if.pw.edu.pl, gabrielw@if.pw.edu.pl

- [1] P. Ring and P. Schuck, *The Nuclear Many-Body Problem* (Springer-Verlag, Berlin, 2000).
- [2] Y.R. Shimizu, J.D. Garrett, R.A. Broglia, M.Gallardo, and E. Vigezzi, Pairing fluctuations in rapidly rotating nuclei, *Rev. Mod. Phys.* **61**, 131 (1989).
- [3] M. Bender, P-H. Heenen, and P-G. Reinhard, Self-consistent mean-field models for nuclear structure, *Rev. Mod. Phys.* **75**, 121 (2003).
- [4] D.J. Dean and M. Hjorth-Jensen, Pairing in nuclear systems: from neutron stars to finite nuclei, *Rev. Mod. Phys.* **75**, 607 (2003).
- [5] Y. Hashimoto, Time-dependent Hartree-Fock-Bogoliubov calculations using a Lagrange mesh with the Gogny interaction, *Phys. Rev. C* **88**, 034307 (2013).
- [6] E. Fonda, D.P. Meichle, N.T. Ouellette, S. Hormoz, and D.P. Lathrop, Direct observation of Kelvin waves excited by quantized vortex reconnection, *Proc. Natl. Acad. Sci. U.S.A.* **111**, 4707 (2014).
- [7] M.J.H. Ku, W. Ji, B. Mukherjee, E. Guardado-Sanchez, L. W. Cheuk, T. Yefsah, and M. W. Zwierlein, Motion of a Solitonic Vortex in the BEC-BCS Crossover, *Phys. Rev. Lett.* **113**, 065301 (2014).
- [8] M.J.H. Ku, B. Mukherjee, T. Yefsah, and M.W. Zwierlein, Cascade of Solitonic Excitations in a Superfluid Fermi gas: From Planar Solitons to Vortex Rings and Lines, *Phys. Rev. Lett.* **116**, 045304 (2016).
- [9] A. Bulgac, M.M. Forbes, M.M. Kelley, K.J. Roche, and G. Wlazłowski, Quantized Superfluid Vortex Rings in the Unitary Fermi Gas, *Phys. Rev. Lett.* **112**, 025301 (2014).
- [10] G. Wlazłowski, A. Bulgac, M.M. Forbes, and K.J. Roche, Life Cycle of Superfluid Vortices and quantum turbulence in the Unitary Fermi Gas, *Phys. Rev. A* **91**, 031602(R) (2015).
- [11] *The BCS-BEC Crossover and the Unitary Fermi Gas*, Lecture Notes in Physics **836**, ed. W. Zwerger, (Springer-Heidelberg 2012).
- [12] G.F. Bertsch, The nuclear density of states in the space of nuclear shapes, *Phys. Lett.* **B95**, 157 (1980).
- [13] F. Barranco, G.F. Bertsch, R.A. Broglia, and E. Vigezzi, Large-amplitude motion in superfluid Fermi droplets, *Nucl. Phys.* **A512**, 253 (1990).
- [14] G.F. Bertsch, Large amplitude collective motion, *Nucl. Phys.* **A574**, 169c (1994).
- [15] A. Bulgac, P. Magierski, K.J. Roche, and I. Stetcu, Induced Fission of  $^{240}\text{Pu}$  within a Real-Time Microscopic Framework, *Phys. Rev. Lett.* **116**, 122504 (2016).
- [16] D.M. Brink, R.A. Broglia, *Nuclear Superfluidity: Pairing in Finite Systems*, Cambridge University Press 2005.
- [17] See Supplemental Material at {URL will be provided by the publisher} for discussion of technical aspects including generation of initial configurations, derivation of energy of the junction, supplemental results, and list of movies, which includes Refs. [18–28].
- [18] G. Wlazowski, K. Sekizawa, P. Magierski, A. Bulgac, M.M. Forbes, Vortex pinning and dynamics in the neutron star crust, *Phys. Rev. Lett.* **117**, 232701 (2016).
- [19] Yongle Yu and Aurel Bulgac, Energy Density Functional Approach to Superfluid Nuclei, *Phys. Rev. Lett.* **90**, 222501 (2003).
- [20] A. Bulgac and Y. Yu, Renormalization of the Hartree-Fock-Bogoliubov Equations in the Case of a Zero Range Pairing Interaction, *Phys. Rev. Lett.* **88**, 042504 (2002).
- [21] A. Bulgac, Local Density Approximation for Systems with Pairing Correlations, *Phys. Rev. C* **65** 051305(R) (2002).
- [22] S. Jin, A. Bulgac, K. Roche, and G. Wlazłowski, Coordinate-Space Solver for Superfluid Many-Fermion Systems with Shifted Conjugate Orthogonal Conjugate Gradient Method, *Phys. Rev. C* **95**, 044302 (2017).
- [23] R. Bass, Fusion of heavy nuclei in a classical model, *Nucl. Phys.* **A231**, 45 (1974).
- [24] C. Golabek and C. Simenel, Collision dynamics of two  $^{238}\text{U}$  atomic nuclei, *Phys. Rev. Lett.* **103**, 042701 (2009).
- [25] C. Bloch and A. Messiah, The canonical form of an antisymmetric tensor and its application to the theory of superconductivity, *Nucl. Phys.* **39**, 95 (1962).
- [26] B. Zumino, Normal Forms of Complex Matrices, *J. Math. Phys.* **3**, 1055 (1962).
- [27] G. Scamps, D. Lacroix, G.F. Bertsch, and K. Washiyama, Pairing dynamics in particle transport, *Phys. Rev. C* **85**, 034328 (2012).
- [28] S. Ebata, T. Nakatsukasa, T. Inakura, K. Yoshida, Y. Hashimoto, and K. Yabana, Canonical-basis time-dependent Hartree-Fock-Bogoliubov theory and linear-

- response calculations, Phys. Rev. C **82**, 034306 (2010).
- [29] K. Dietrich, On a nuclear Josephson effect in heavy ion scattering, Phys. Lett. **B32**, 428 (1970).
- [30] K. Dietrich, Semiclassical Theory of a Nuclear Josephson Effect in Reactions between Heavy Ions, Ann. Phys. (N.Y.) **66**, 480, (1970).
- [31] K. Dietrich, K. Hara, and F. Weller, Multiple pair transfer in reactions between heavy nuclei, Phys. Lett. **B35**, 201 (1971).
- [32] J. H., Sorensen and A. Winther, Multipair transfer in collisions between heavy nuclei, Phys. Rev. C **47**, 1691 (1993).
- [33] Y. Hashimoto and G. Scamps, Gauge angle dependence in TDHFB calculations of  $^{20}\text{O}+^{20}\text{O}$  head-on collisions with the Gogny interaction, Phys. Rev. C **94**, 014610 (2016).
- [34] L. N. Oliveira, E. K. U. Gross, and W. Kohn, Density-Functional Theory for Superconductors, Phys. Rev. Lett. **60**, 2430 (1988).
- [35] O. -J. Wacker, R. Kümmel, and E. K. U. Gross, Time-Dependent Density-Functional Theory for Superconductors, Phys. Rev. Lett. **73**, 2915 (1994).
- [36] A. Bulgac and S. Yoon, Large Amplitude Dynamics of the Pairing Correlations in a Unitary Fermi Gas, Phys. Rev. Lett. **102**, 085302 (2009).
- [37] A. Bulgac, Y.-L. Luo, P. Magierski, K.J. Roche, and Y. Yu, Real-Time Dynamics of Quantized Vortices in a Unitary Fermi Superfluid, Science **332**, 1288 (2011).
- [38] A. Bulgac, P. Magierski, and M.M. Forbes, The Unitary Fermi Gas: From Monte Carlo to Density Functionals, in *BCS-BEC Crossover and the Unitary Fermi Gas*, edited by W. Zwerger, Lecture Notes in Physics, Vol. **836**, pp 305-373 (Springer, Heidelberg, 2012).
- [39] A. Bulgac, Y.-L. Luo, and K.J. Roche, Quantum Shock Waves and Domain Walls in Real-Time Dynamics of a Superfluid Unitary Fermi Gas, Phys. Rev. Lett. **108**, 150401 (2012).
- [40] A. Bulgac, Time-Dependent Density Functional Theory and Real-Time Dynamics of Fermi Superfluids, Ann. Rev. Nucl. Part. Sci. **63**, 97 (2013).
- [41] I. Stetcu, A. Bulgac, P. Magierski, and K.J. Roche, Isovector Giant Dipole Resonance from 3D Time-Dependent Density Functional Theory for Superfluid Nuclei, Phys. Rev. C **84**, 051309(R) (2011).
- [42] I. Stetcu, C.A. Bertulani, A. Bulgac, P. Magierski, and K.J. Roche, Relativistic Coulomb Excitation within Time-Dependent Superfluid Local Density Approximation, Phys. Rev. Lett. **114**, 012701 (2015).
- [43] P. Magierski, Nuclear Reactions and Superfluid Time Dependent Density Functional Theory, invited paper honoring Prof. Joachim Maruhn's retirement to be published as a chapter in "Progress of time-dependent nuclear reaction theory" (ed. Yoritaka Iwata) in the ebook series: "Frontiers in nuclear and particle physics" (Bentham Science Publishers); arXiv:1606.02225.
- [44] S.A. Fayans, Towards a universal nuclear density functional, JETP Letters **68**, 169 (1998).
- [45] S.A. Fayans, S.V. Tolokonnikov, E.L. Trykov, and D. Zawischa, Nuclear isotope shifts within the local energy-density functional approach, Nucl. Phys. **A676**, 49 (2000).
- [46] K. Sekizawa, P. Magierski, and G. Wlazłowski, Solitonic Excitations in Collisions of Superfluid Nuclei, arXiv:1702.00069 (2017).
- [47] Y. Nambu, Quasi-Particles and Gauge Invariance in the Theory of Superconductivity, Phys. Rev. **117**, 648 (1960).
- [48] J. Goldstone, Field theories with «Superconductor» solutions, Il Nuovo Cimento **19**, 154 (1961).
- [49] T. Nakatsukasa, K. Matsuyanagi, M. Matsuo, and K. Yabana, Time-dependent density-functional description of nuclear dynamics, Rev. Mod. Phys. **88**, 045004 (2016).
- [50] We thank Aurel Bulgac for pointing it to us.
- [51] J.F. Liang, C.J. Gross, Z. Kohley, D. Shapira, R.L. Varner, J.M. Allmond, A.L. Caraley, K. Lagergren, and P. E. Mueller, Fusion probability for neutron-rich radioactive-Sn-induced reactions, Phys. Rev. C **85** 031601, (2012).
- [52] C.C. Sahn, H.G. Clerc, K.-H. Schmidt, W. Reisdorf, P. Armbruster, F.P. Hessberger, J.G. Keller, G. Münzenberg, D. Vermeulen, Fusion probability of symmetric heavy, nuclear systems determined from evaporation-residue cross sections, Nucl. Phys. **A441**, 316 (1985).
- [53] W.J. Swiatecki, The dynamics of the fusion of two nuclei, Nucl. Phys. **A376**, 275 (1982).
- [54] S. Bjornholm and W.J. Swiatecki, Dynamical aspects of nucleus-nucleus collisions, Nucl. Phys. **A391**, 471 (1982).
- [55] R. Donangelo, L.F. Canto, Studies of nucleus-nucleus collisions with a schematic liquid-drop model and one-body dissipation, Nucl. Phys. **A451**, 349 (1986).
- [56] K. Washiyama, Microscopic analysis of fusion hindrance in heavy nuclear systems, Phys. Rev. C **91**, 064607 (2015).
- [57] G. Scamps and D. Lacroix, Effect of pairing on one- and two-nucleon transfer below the Coulomb barrier: A time-dependent microscopic description, Phys. Rev. C **87**, 014605 (2013).
- [58] G. Scamps and D. Lacroix, Effect of pairing on transfer and fusion reactions, EPJ Web of Conf. **86**, 00042 (2015).
- [59] S. Ebata and T. Nakatsukasa, Repulsive Aspects of Pairing Correlation in Nuclear Fusion Reaction, JPS Conf. Proc. **6**, 020056 (2015).
- [60] A. Bulgac and S. Jin, Dynamics of Fragmented Condensates and Macroscopic Entanglement, Phys. Rev. Lett. (to be published), arXiv:1701.06683



**Supplemental online material for:  
“Novel Role of Superfluidity in Low-Energy  
Nuclear Reactions”**

In this supplemental material, we describe technical aspects related to: generation of the initial configurations, setting initial conditions for a collision and extracting kinetic energy of the fragments after collision. We also provide the evaluation of the contact energy of two superfluids within the Ginzburg-Landau theory and the classical fusion cross section taking into account nonzero phase differences between nuclear pairing fields. We show results of  $^{240}\text{Pu}+^{240}\text{Pu}$  with  $\Delta\varphi_p \neq \Delta\varphi_n$  quantifying contributions from neutrons and protons, and with ternary quasifission processes. We also present typical results for asymmetric collisions of  $^{86}\text{Zr}+^{126}\text{Sn}$  and non-central collisions of  $^{90}\text{Zr}+^{90}\text{Zr}$ . Finally, the difference between TDHF+BCS and TDHFB approaches is clarified. Description of various supplemental movies is given.

**TDSLDA CALCULATIONS FOR NUCLEAR  
REACTIONS**

In this section we present the methodology which has been applied in order to:

- prepare initial configurations with two spatially separated nuclei,
- imprint the phase difference of the pairing fields of the two nuclei,
- collide them to simulate nuclear reactions within the framework of TDSLDA.

The initial states for the TDSLDA calculations were obtained as self-consistent solutions of the static SLDA equations which for both protons and neutrons have the following structure:

$$\begin{pmatrix} h - \mu & \Delta \\ \Delta^* & -(h^* - \mu) \end{pmatrix} \begin{pmatrix} u_k \\ v_k \end{pmatrix} = \varepsilon_k \begin{pmatrix} u_k \\ v_k \end{pmatrix}, \quad (2)$$

where  $h$  is the single-particle Hamiltonian and  $\Delta$  is the pairing field, which are defined by functional derivatives of an energy density functional, and  $\mu$  is the chemical potential (for either protons or neutrons). To reduce the number of diagonalizations needed to get the self-consistent solution, we have used the procedure similar to the one adopted to compute initial states for a vortex-nucleus system in the neutron star crust [1]. The lattice size is  $64 \times 20 \times 20$  for head-on collisions and  $64 \times 48 \times 20$  for non-central collisions. The lattice spacing is 1.25 fm. The pairing part of the density functional has a local form,  $\mathcal{E}_{\text{pair}}(\mathbf{r}) = g[|\nu_n(\mathbf{r})|^2 + |\nu_p(\mathbf{r})|^2]$ , where  $\nu_{p,n}$  are proton and neutron anomalous densities and the coupling constant was set to  $g = -200 \text{ MeV fm}^3$  [2]. It corresponds to the zero-range pairing force which needs to be regularized. We use the procedure described in Refs. [3, 4].

After the regularization the pairing field is given by  $\Delta_{n,p}(\mathbf{r}) = -g_{\text{eff}}\nu_{n,p}(\mathbf{r})$ , where  $g_{\text{eff}}$  is the effective coupling constant and  $\nu_{n,p}$  is computed in the restricted quasiparticle space with cutoff energy,  $E_{\text{cut}} = 100 \text{ MeV}$ .

One has to keep in mind that  $u$ -components and  $v$ -components, forming quasiparticle wave functions, behave differently when expressed in the coordinate representation. While the  $v$ -components are spatially localized around the two nuclei (as is always true for bound systems), the  $u$ -components are distributed over the whole space. Thus, one has to pay a particular attention when dealing with a system of two spatially separated nuclei, as they are entangled through the common  $u$ -components. For example, a discontinuity of the  $u$ -components is introduced if one generates separately ground states for two nuclei placed in smaller volumes and then combines them together in a larger volume. This is a typical method used in TDHF calculations, which is justified since the  $u$ - and  $v$ -components are decoupled for  $\Delta = 0$  and one evolves only localized single-particle wave functions. In our case, however, this method is not justified and therefore we generated self-consistent solutions for two nuclei within a single box separated by a desired distance  $\Delta x \approx 50 \text{ fm}$ . In order to avoid two nuclei to move apart because of the Coulomb repulsion, we have introduced an external potential:

$$V_{\text{ext}}(\mathbf{r}) = \sqrt{[V_0(x - x_0)]^2 + \delta^2}, \quad (3)$$

which is uniform in  $y$ - and  $z$ -direction. The parameter  $\delta$  is a small constant which makes  $V_{\text{ext}}$  smooth around the center of the box ( $x_0 = 40 \text{ fm}$ ). Away from the center of the box the external potential is linear  $V_{\text{ext}}(\mathbf{r}) \simeq V_0|x - x_0|$ , and generates the constant force which compensates for the Coulomb repulsion. The parameter  $V_0$  is adjusted to keep the two nuclei at rest during the self-consistent iterations. An example of the potential  $V_{\text{ext}}$  is shown in Fig. 5 (a). We used a shifted conjugate orthogonal conjugate gradient (COCG) method to compute densities during iterations [5]. Subsequently a direct diagonalization of the Hamiltonian (2) was performed, which provided the wave functions determining the initial configuration for both the projectile and the target nuclei contained in the common simulation box.

The generated initial states are characterized by the pairing field that has the uniform phase over the box. One can change the phase of one of the nuclei without affecting the energy of the system. This can be done dynamically, using the phase imprint technique commonly used in experiments on ultracold atomic gases. Namely, the additional external potential is applied for a certain time interval  $t_p$ . The external potential has the following

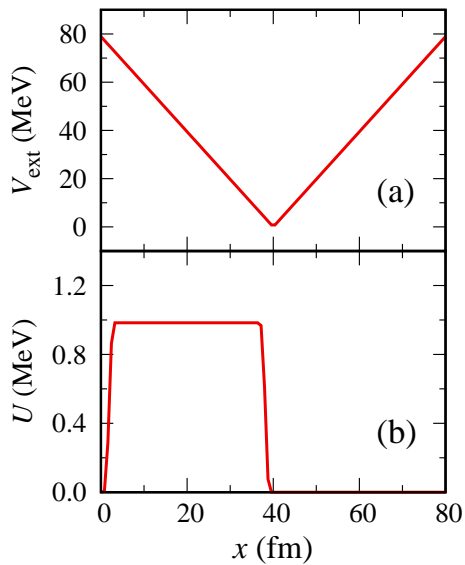


FIG. 5: An example of external potentials used for keeping nuclei at rest or for accelerating them (a) and for imprinting the required phase difference (b) as a function of  $x$  coordinate (along the collision axis). (a)  $V_{\text{ext}}$  defined by Eq. (3) is shown for  $V_0/\hbar c = 10^{-4} \text{ fm}^{-1}$  and  $\delta/\hbar c = 0.0003 \text{ fm}^{-1}$ . (b)  $U$  defined by Eq. (4) is shown for the case of imprinting the phase difference  $\Delta\varphi = \pi$  during the time interval  $1000 \text{ fm}/c$ .

form:

$$U(\mathbf{r}) = \begin{cases} U_0 s(x, 3.75, 2), & x \leq 3.75, \\ U_0, & 3.75 < x < 36.25, \\ U_0 s(x - 36.25, 3.75, 2), & 36.25 \leq x < 40, \\ 0, & x \geq 40, \end{cases} \quad (4)$$

where  $s(x, w, \alpha)$  is a function which smoothly varies from 0 to 1 in an interval  $[0, w]$ :

$$s(x, w, \alpha) = \frac{1}{2} + \frac{1}{2} \tanh \left[ \alpha \tan \left( \frac{\pi x}{w} - \frac{\pi}{2} \right) \right]. \quad (5)$$

An example of the potential is shown in Fig. 5 (b). Since the pairing field is proportional to the anomalous density  $\nu = \sum_{0 < E_n < E_{\text{cut}}} u_n v_n^*$ , the phase of the pairing field for the left half of the box ( $x < 40 \text{ fm}$ ) evolves in time as  $\Delta(\mathbf{r}, t) = e^{2i(\mu - U_0)t/\hbar} |\Delta(\mathbf{r}, t)|$ , whereas for the right half ( $x > 40 \text{ fm}$ ) it evolves as  $\Delta(\mathbf{r}, t) = e^{2i\mu t/\hbar} |\Delta(\mathbf{r}, t)|$ . Consequently after time  $t_p$  the phase for one side gets an extra shift  $\Delta\varphi = 2U_0 t_p/\hbar$ . The height of the potential  $U_0$  is adjusted to introduce the requested phase difference  $\Delta\varphi$  within a time interval  $t_p = 1000 \text{ fm}/c$ .

Finally, to collide two nuclei one needs to accelerate them up to a certain value of relative velocity. It is achieved by varying smoothly the slope parameter  $V_0$  in Eq. (3) to a larger value  $V_1 (> V_0)$  using the switching function. It is performed in a relatively short time of about  $10 \text{ fm}/c$ . Subsequently, the slope parameter  $V_1$  is kept fixed until the two nuclei reach the desired relative

velocity. Once this velocity is reached the external potential (3) is switched off (within the time of  $10 \text{ fm}/c$ ), and the two nuclei collide. The collision energy is defined at the time when  $V_{\text{ext}}$  becomes zero.

## ENERGY OF THE JUNCTION

Let us consider two superfluids being in contact and having the same superfluid density  $n_s$ , differing only by the phase of the order parameter  $\varphi_{1,2}$  (see Fig. 6).

The energy of the junction is associated with the spatial variations of the phase on the length scale defined by the contact size. It can be easily evaluated within the Ginzburg-Landau (G-L) approach. This is a macroscopic theory that describes evolution of the order parameter of a superfluid. The only requirement is that the system is characterized by a complex order parameter. Namely, one can introduce the wave function of the condensate  $\Psi(\mathbf{r})$  which is related to the superfluid order parameter with  $|\Psi|^2$  being the density of particles that belong to the condensate. This quantity will be temperature dependent and clearly vanishes at critical temperature  $T = T_c$ . Superfluidity in fermionic systems is regarded as a condensate of Cooper pairs, thus  $2|\Psi|^2$  has meaning of fermionic density. Consequently, the wave function is expressed as

$$\Psi(\mathbf{r}) = \sqrt{\frac{n_s(\mathbf{r})}{2}} e^{i\varphi(\mathbf{r})}, \quad (6)$$

where  $n_s \propto (1 - T/T_c)$  is the superfluid density of fermions, and  $\varphi$  denotes the phase. In general the total density of particles separates into superfluid and normal components  $n = n_s + n_n$  and in the zero temperature limit the latter vanishes. The total free energy of the system is given by

$$F_{\text{tot}} = \int (F_L(\mathbf{r}) + F_{\text{grad}}(\mathbf{r})) d\mathbf{r}, \quad (7)$$

where  $F_L = \alpha(T)|\Psi(\mathbf{r})|^2 + \beta(T)|\Psi(\mathbf{r})|^4$  is the so-called Landau term. Information about type of system is encapsulated in coupling constants appearing in this term. Since superfluid densities of both superfluids are equal this term does not contribute to the free energy of the junction. What matters is the gradient term which has the form:

$$F_{\text{grad}} = \frac{\hbar^2}{2m^*} |\nabla\Psi(\mathbf{r})|^2, \quad (8)$$

where  $m^*$  is the effective mass of particles that form the condensate, and we assume  $m^* = 2m_n$  which is the mass of the Cooper pair ( $m_n$  is the nucleon mass). Approximating the gradient by

$$\nabla\Psi(\mathbf{r}) \approx \sqrt{\frac{n_s}{2}} \frac{e^{i\varphi_2} - e^{i\varphi_1}}{L}, \quad (9)$$



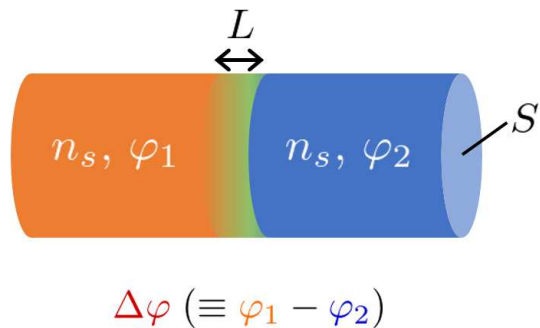


FIG. 6: Schematic picture of a junction of two superfluids with different phases. This picture illustrates those quantities which enters Eq. (11):  $S$  is the area of the junction,  $L$  is the length scale over which the phase varies,  $n_s$  is the superfluid density, and  $\varphi_i$  ( $i = 1, 2$ ) is the phase of the pairing field.

where  $L$  is the length scale over which the phase varies from value  $\varphi_1$  to  $\varphi_2$ , one finds the free energy of the junction (see also Fig. 6):

$$F_j = \frac{S}{L} \frac{\hbar^2}{2m_n} n_s \sin^2 \frac{\Delta\varphi}{2}, \quad (10)$$

where we have applied  $|e^{i\varphi_2} - e^{i\varphi_1}|^2 = 4 \sin^2 \frac{\Delta\varphi}{2}$ , denoting  $\Delta\varphi = \varphi_1 - \varphi_2$  and  $SL$  is the volume of the junction. In the zero temperature limit the free energy becomes the energy of the junction and the superfluid density  $n_s$  becomes neutrons/protons density:

$$E_j = \frac{S}{L} \frac{\hbar^2}{2m_n} n_s \sin^2 \frac{\Delta\varphi}{2}. \quad (11)$$

For a collision of two heavy nuclei at energies close to the Coulomb barrier, one may assume the area of the junction  $S$  corresponds to the neck, which is on the order of  $\pi R^2$  with  $R \approx 6$  fm, and taking  $L \approx R$  and  $n_s$  as a half of nuclear density, one finds that the energy of the junction varies by several tens of MeV

## PHASE EVOLUTION IN A COLLIDING SYSTEM

In this section we provide information about time evolution of the phase of the pairing field during a collision. In Fig. 7, we show the phase evolution for the  $^{240}\text{Pu} + ^{240}\text{Pu}$  reaction at  $E \simeq 1.1V_{\text{Bass}}$ , as a typical example. These snapshots correspond precisely to the frames shown in Fig. 2 of the main text. Two extreme cases corresponding to the relative phase  $\Delta\varphi = 0$  (left column) and  $\pi$  (right column) are shown. Note that these values specify the phase difference for the initial state, where two nuclei are far away from each other. The uniformity of the phase across the nuclei is destroyed by the accelerating potential, see Eq. (4) and Fig. 5 (a). For this reason before collision the phase varies along the collision axis inside each nucleus, see top two panels of Fig. 7. The phase

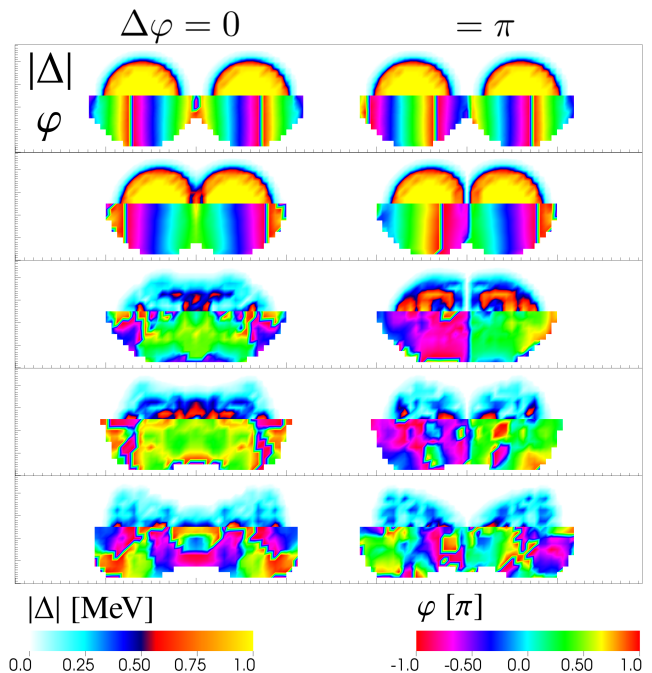


FIG. 7: Evolution of the neutron pairing field  $\Delta(\mathbf{r}) = |\Delta(\mathbf{r})|e^{i\varphi(\mathbf{r})}$  for the  $^{240}\text{Pu} + ^{240}\text{Pu}$  reaction at  $E \simeq 1.1V_{\text{Bass}}$ . Upper-half of each panel shows absolute value  $|\Delta(\mathbf{r})|$ , while lower-half presents the phase  $\varphi(\mathbf{r})$ . Left column corresponds to the case without relative phase difference between colliding nuclei in the initial state ( $\Delta\varphi = 0$ ), while right column corresponds to the extreme case where the phase difference is the largest ( $\Delta\varphi = \pi$ ).

relaxes fast, and when two nuclei collide and merge, one can easily define domains with well defined phase, as seen on middle panels of the figure. Finally, when the composite system splits into two fragments, the phase pattern starts to be disordered. One should note, however, that due to large excitations in this violent collision, the neutron pairing is also substantially destroyed (cf. upper-half of each panel of the figure).

## KINETIC ENERGY OF THE FRAGMENTS

The total kinetic energy (TKE) of the outgoing fragments is evaluated as follows. We divide the simulation box into two regions by a plane parallel to the  $yz$ -plane, which defines left ( $x < 40$  fm) and right ( $x > 40$  fm) regions. Subsequently we compute the average mass and charge numbers and the center-of-mass of the fragments in respective regions,  $A_{L,R}$ ,  $Z_{L,R}$  and  $\mathbf{R}_{L,R}(t)$ . From the time derivative of the relative distance  $\mathbf{R}(t) = \mathbf{R}_R(t) - \mathbf{R}_L(t)$ , we compute the relative velocity  $\mathbf{V}(t)$ . We compute the TKE of the fragments when they are well separated spatially ( $R \simeq 30$  fm) as

follows:

$$\text{TKE} = \frac{1}{2}\mu(t)\mathbf{V}^2(t) + \frac{Z_L(t)Z_R(t)e^2}{|\mathbf{R}(t)|}, \quad (12)$$

where  $\mu(t) = m_n A_L(t)A_R(t)/(A_L(t) + A_R(t))$  with  $m_n$  being the nucleon mass. To check the validity of this simple formula (12), we have also computed the TKE as follows:

$$\text{TKE} = \frac{\mathbf{P}_L^2}{2M_L(t)} + \frac{\mathbf{P}_R^2}{2M_R(t)} + V_{\text{Coul}}(t), \quad (13)$$

where  $M_{L(R)}(t) = m_n A_{L(R)}(t)$ , and the momentum is defined by

$$\mathbf{P}_{L(R)} = m_n \int_{L(R)} \mathbf{j}(\mathbf{r}, t) d\mathbf{r}. \quad (14)$$

The Coulomb energy can be evaluated from the proton density:

$$V_{\text{Coul}}(t) = e^2 \int_L \int_R \frac{\rho_p(\mathbf{r}_1, t)\rho_p(\mathbf{r}_2, t)}{|\mathbf{r}_1 - \mathbf{r}_2|} d\mathbf{r}_1 d\mathbf{r}_2. \quad (15)$$

We have found that the difference between Eqs. (12) and (13) is very small, at most a few MeV at certain times where fragments are close to each other and exhibit large deformations, where multipole corrections play a role.

## EFFECTS ON FUSION CROSS SECTION

The effect of the increased barrier can be included in the expression for the classical fusion cross section. Namely, the classical expression reads:

$$\sigma(E) = \pi R^2 \left(1 - \frac{B}{E}\right) \quad (16)$$

where  $B$  defines the barrier height and  $E > B$ . The modification of this expression related to the pairing field phase difference reads:

$$\sigma(E) = R^2 \left( \Delta\varphi_{\text{th}}(E) - \frac{1}{E} \int_0^{\Delta\varphi_{\text{th}}(E)} B(\Delta\varphi) d(\Delta\varphi) \right), \quad (17)$$

where  $R = r_0(A_1^{1/3} + A_2^{1/3})$  with  $r_0 \approx 1.25$  fm, and  $\Delta\varphi_{\text{th}}$  is the threshold phase difference below which the capture occurs at a given collision energy  $E$ . The expression requires  $E \geq E_{\text{min}}$ , where  $E_{\text{min}}$  is the lowest energy for capture without phase difference, *i.e.*,  $\Delta\varphi_{\text{th}}(E_{\text{min}}) = 0$ . One can easily notice that for  $E > E_{\text{max}}$ , where  $\Delta\varphi_{\text{th}}(E_{\text{max}}) = \pi$ , the above formula is consistent with Eq. (16), with barrier height averaged over all angles:  $\bar{B} = \frac{1}{\pi} \int_0^\pi B(\Delta\varphi) d(\Delta\varphi)$ . Thus the effect of the phase difference on the fusion cross section will enter through the effective barrier height averaged over all phase differences. In the energy interval  $E_{\text{min}} < E < E_{\text{max}}$  one may

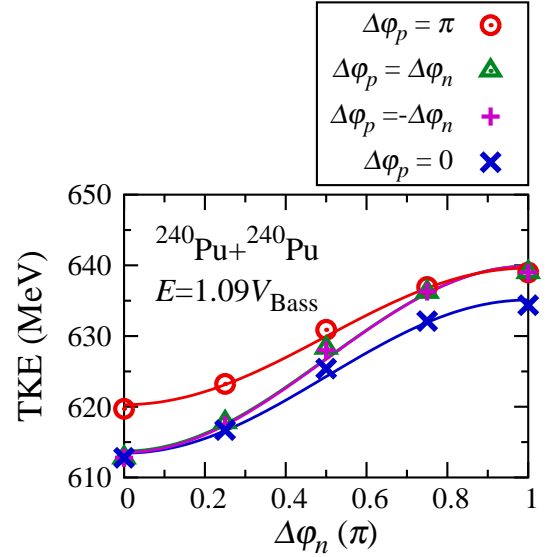


FIG. 8: Total kinetic energy (TKE) of outgoing fragments in  $^{240}\text{Pu}+^{240}\text{Pu}$  collisions at  $E \simeq 1.09V_{\text{Bass}}$  as a function of the pairing phase difference for neutron superfluids,  $\Delta\varphi_n$ . The four different symbols correspond to the following cases: green open triangles denote results obtained under condition that the imprinted phase difference for both neutron and proton superfluids is the same:  $\Delta\varphi_p = \Delta\varphi_n = \Delta\varphi$  (This case has been shown in Fig. 3 (a) of the main text); pink plus symbols correspond to the case of proton superfluids having the opposite phase difference to that of neutron superfluids:  $\Delta\varphi_p = -\Delta\varphi_n$ ; red open circles (blue crosses) correspond to the case of proton superfluids having the fixed phase difference at values:  $\Delta\varphi_p = \pi$  (0). The solid curves represent fits to the data points with the expression  $\alpha + \beta \sin^2 \frac{\Delta\varphi_n}{2}$ , taking  $\alpha$  and  $\beta$  as parameters.

use the above formula to extract energy dependence of  $\Delta\varphi_{\text{th}}$ , directly from the excitation function, namely,

$$\frac{1}{R^2} \frac{d}{dE} (E\sigma(E)) = \Delta\varphi_{\text{th}}(E). \quad (18)$$

In practice, however, this quantity will be contaminated by other effects like, *e.g.*, quantum tunneling and nonzero width of the barrier distribution.

## THE CASE OF $\Delta\varphi_p \neq \Delta\varphi_n$

In order to investigate the magnitude of contributions coming from proton and neutron superfluids separately, we have performed simulations of head-on collisions of  $^{240}\text{Pu}+^{240}\text{Pu}$  with different relative phases of proton and neutron pairing fields, *i.e.*  $\Delta\varphi_p \neq \Delta\varphi_n$ .

Let us first focus on the TKE of the fragments. In Fig. 8, we show the TKE as a function of the pairing phase difference for neutron superfluids,  $\Delta\varphi_n$ . The collision energy was set to  $E \simeq 1.09V_{\text{Bass}}$ , at which we have observed the most pronounced effect generating the

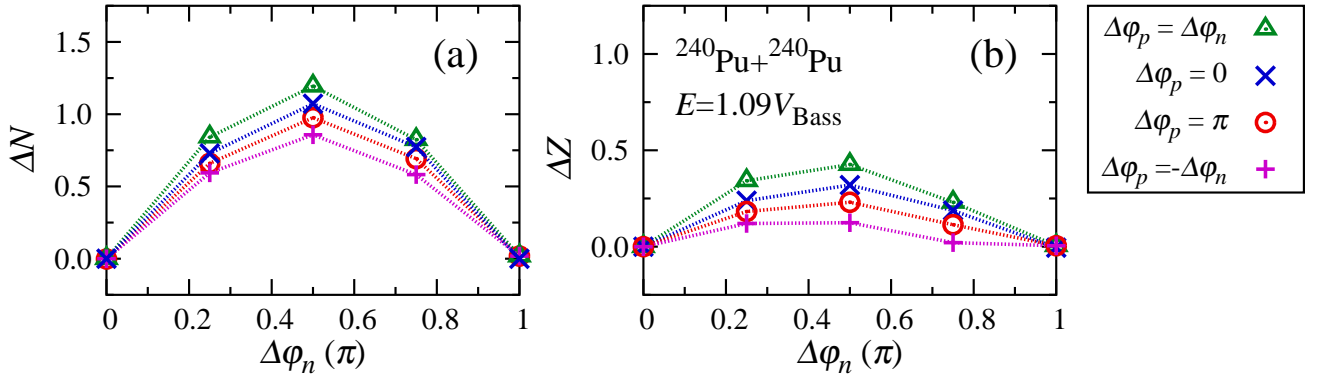


FIG. 9: Average number of transferred neutrons (a) and protons (b) from the left to the right regions in  $^{240}\text{Pu}+^{240}\text{Pu}$  collisions at  $E \simeq 1.09V_{\text{Bass}}$  for various types of phase differences. The horizontal axis is the pairing phase difference for neutron superfluids,  $\Delta\varphi_n$ . Green open triangles show results where the phase is imprinted for both neutrons and protons the same amount ( $\Delta\varphi_p = \Delta\varphi_n = \Delta\varphi$ ) (The same results as shown in Fig. 3 (b) of the main text). Pink plus symbols correspond to the cases where the phase difference for protons is opposite to that for neutrons ( $\Delta\varphi_p = -\Delta\varphi_n$ ). Red open circles (blue crosses) correspond to the cases where the phase difference for protons is fixed to  $\Delta\varphi_p = \pi$  (0).

largest TKE differences of about 25 MeV (see Fig. 3 (a) in the main text). The quantity  $V_{\text{Bass}}$  is the phenomenological fusion barrier [6].

In the figure one can see four curves representing TKE( $\Delta\varphi_n$ ), although two of them ( $\Delta\varphi_p = \pm\Delta\varphi_n$  cases) practically coincide. It indicates that the effect governing the TKE behavior is related to the solitonic excitation, as the energy of the junction is the same in the two cases. This fact also confirms that the effects related to Josephson currents are indeed negligible, since in the case of  $\Delta\varphi_p = \Delta\varphi_n$  protons and neutrons are transferred in the same direction, whereas in the case of  $\Delta\varphi_p = -\Delta\varphi_n$  the directions of induced currents for protons and neutrons are opposite. The other two curves correspond to  $\Delta\varphi_p = \pi$  and  $\Delta\varphi_p = 0$  cases. The relative energy shift of these curves measures the magnitude of the contribution coming from the pairing phase difference for protons. Thus, clearly the total effect reflected in TKE comes from both proton and neutron superfluids, however the neutron contribution ( $\approx 21$  MeV) is significantly larger than the proton contribution ( $\approx 4-7$  MeV). This we attribute to the fact that neutrons play more important role in the neck formation, whereas contribution of protons is effectively suppressed by the Coulomb repulsion.

In Fig. 9, we show the average number of transferred neutrons (a) and protons (b) from the left nucleus to the right one as a function of the pairing phase difference for neutrons,  $\Delta\varphi_n$ . All symbols are the same as in Fig. 8. In particular, green open triangles shown in Fig. 9 (a) denote the results shown also in Fig. 3 (b) of the main text. The amount of nucleons transferred during the collisions is the largest for the case of  $\Delta\varphi_p = \Delta\varphi_n$ , *i.e.*, the case where both protons and neutrons flow in the same direction. On the other hand, in the case of  $\Delta\varphi_p = -\Delta\varphi_n$  the amount of transferred nucleons is the smallest, since induced currents for protons and neutrons have the op-

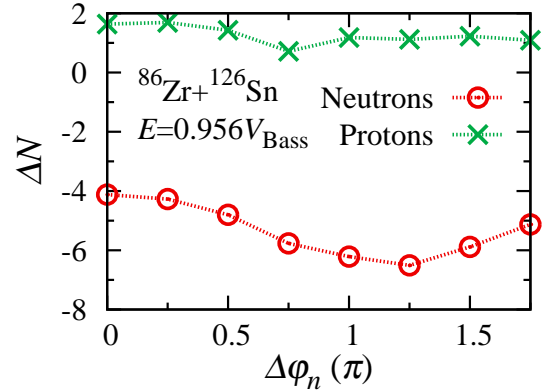


FIG. 10: Average number of transferred neutrons (red circles) and protons (green crosses) in an asymmetric reaction,  $^{86}\text{Zr}+^{126}\text{Sn}$ , at an energy below the fusion threshold ( $E = 0.956V_{\text{Bass}}$ ) as a function of phase differences for the neutron pairing field,  $\Delta\varphi_n$ , in the initial state.

posite directions, and due to the mutual entrainment the magnitude of the currents is suppressed. Moreover, one can find a visible difference between the cases of  $\Delta\varphi_p = 0$  and  $\Delta\varphi_p = \pi$ , despite the fact that the proton induced current is absent in both cases. It indicates that the solitonic structure in the proton pairing field plays also a role of a barrier suppressing neutron flow. Nevertheless in both cases ( $\Delta\varphi_p = 0, \pi$ ) a small number of protons are transferred, it is only due to the neutron induced current which entrain protons.

## ASYMMETRIC REACTIONS

To examine the effects of the pairing phase difference on the dynamics in asymmetric reactions, we performed

exploratory calculations for  $^{86}\text{Zr}+^{126}\text{Sn}$ . In these reactions the phase difference is not a well-defined quantity, but it evolves in time and the evolution rate is determined by the difference of the nuclear chemical potentials. In the case of symmetric reactions (like  $^{90}\text{Zr}+^{90}\text{Zr}$ ) the collisions for the phase differences  $\Delta\varphi$  and  $2\pi - \Delta\varphi$ , are connected by reflection symmetry (*i.e.* the symmetry under an exchange of the colliding nuclei) and therefore the relevant range for the phase difference is limited to the interval  $[0, \pi]$ . This is no longer correct for asymmetric reactions and one has to consider all phase differences that span interval  $\Delta\varphi \in [0, 2\pi]$ . Nevertheless, we have observed qualitatively the same effect of the barrier enhancement due to the pairing as in  $^{90}\text{Zr}+^{90}\text{Zr}$  reactions.

For the asymmetric reaction, at energy below the fusion threshold, the natural process that takes place is the particle transfer (due to difference in the chemical potentials). We observed that the phase difference can modify the amount of nucleon transfer. As an example in Fig. 10 we show the particle transfer for various phase differences of the initial state. Depending on the relative phase of the pairing fields, 4–6 neutrons are transferred. The fluctuations in the particle transfer are about 2 particles, thus very similar to the other cases. The fluctuation of 2 particles is due to the induced current that can either enhance or suppress the particle flow. The effects also induce indirectly variations for protons transfer (note that  $Z = 40$  is a magic number without spin-orbit coupling and protons in Zr are in normal phase).

### TERNARY QUASIFISSION

In the case of  $^{240}\text{Pu}+^{240}\text{Pu}$  collisions at sufficiently high energies, we have observed exotic reaction dynamics. Namely, at energy  $E \simeq 1.5V_{\text{Bass}}$  the composite system splits producing a third light fragment for all phase differences  $\Delta\varphi$ . Such a ternary quasifission process has been observed as well in TDHF approach [7], indicating the possibility of emission of a light fragment in the collision process. Interestingly, the third fragment is not at rest as it should be in the case of TDHF approach, where the left-right symmetry is being conserved in symmetric collisions in the center-of-mass frame. In our approach, however, the symmetry is broken due to the different phases of pairing fields of incoming nuclei. The induced current appears as a consequence of the symmetry breaking component in the pairing field. Therefore, it is not surprising that the third fragment is not at rest and is moving after splitting due to the current induced by the phase difference. Moreover, at energies  $E \simeq 1.3V_{\text{Bass}}$  and  $E \simeq 1.4V_{\text{Bass}}$ , we have found that the number of fragments is affected by the phase difference. The situation is exhibited in Fig. 11. In this case, the solitonic structure prevents the formation of the third fragment from the neck region. The observed effects implicitly indicate

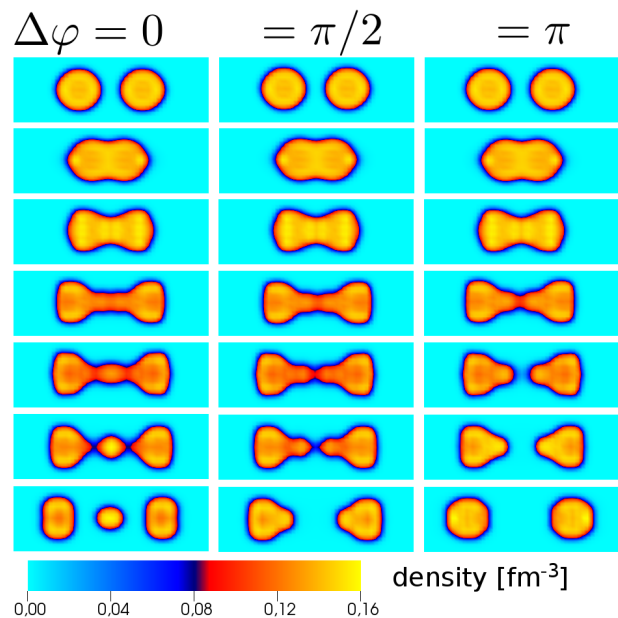


FIG. 11: Snapshots of the density distribution on the reaction plane for  $^{240}\text{Pu}+^{240}\text{Pu}$  collisions at  $E \simeq 1.3V_{\text{Bass}}$ , for three pairing phase differences:  $\Delta\varphi = 0$  (left column),  $\Delta\varphi = \pi/2$  (middle column) and  $\Delta\varphi = \pi$  (right column). Contact time spans the interval 570–650 fm/c depending on the phase difference. A third fragment is created for the phase difference  $\Delta\varphi \lesssim \frac{\pi}{4}$ . For full movie, see 240Pu+240Pu\_1.30V.mp4 (<https://youtu.be/7UstUB6DBn4>).

the importance of the phase difference on the reaction dynamics even at relatively high energies, although one should keep in mind if TDSLDA description for such high energy collisions is valid.

### NON-CENTRAL COLLISIONS

In order to investigate collision trajectories and their dependence on the pairing field phase differences, we have performed collisions with nonzero impact parameters. Since we solve TDSLDA equations in 3D Cartesian coordinates without any symmetry restrictions, we can also simulate non-central collisions. We have performed simulations for non-central collisions of  $^{240}\text{Pu}+^{240}\text{Pu}$  and  $^{90}\text{Zr}+^{90}\text{Zr}$ . Similarly to central collisions, the phase difference prevents superfluid nucleons to enter the neck region. It causes the suppression of the neck formation and consequently the reduction of the contact time. In the non-central collisions, however, the small variations of the contact time have a dramatic effect on the collision trajectories. It affects both the scattering angle as well as kinetic energy of the fragments and induces the correlation between these two quantities at a fixed impact parameter. In Fig. 12, we show an example of the non-central collisions of  $^{90}\text{Zr}+^{90}\text{Zr}$ , where the energy and

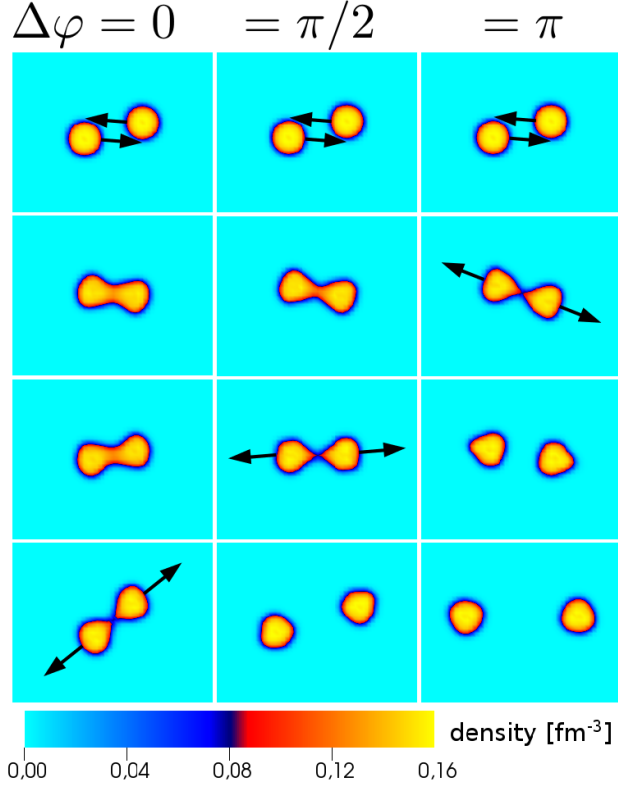


FIG. 12: Snapshots of the density on the reaction plane for non-central collisions of  $^{90}\text{Zr}+^{90}\text{Zr}$  at  $E \simeq 1.4V_{\text{Bass}}$  ( $b \approx 2$  fm), for three pairing phase differences:  $\Delta\varphi = 0$  (left column),  $\Delta\varphi = \pi/2$  (middle column) and  $\Delta\varphi = \pi$  (right column). Contact time depends on the relative phase difference and it is approximately equal to: 1000, 840, and 720 fm/c, for phase differences 0,  $\pi/2$ , and  $\pi$ , respectively. For full movie, see 90Zr+90Zr.noncentral13.1.38V.mp4 (<https://youtu.be/UCCAN9ahNqA>).

the impact parameter are chosen in a such way that the system does not fuse, but splits after certain time. As is apparent from the figure, the pairing phase difference affects the contact time and consequently the scattering angles.

### TDHF+BCS VS. TDHFB

In this section we demonstrate the effects that are triggered by pairing field dynamics, like studied in this Letter, cannot be investigated within TDHF+BCS framework.

Let us begin with the static description. The difference between BCS and HFB treatments can be formally expressed on the level of the Bloch-Messiah-Zumino (BMZ) decomposition of the Bogoliubov transform [8, 9]. Namely, the BCS approach assumes that the third transform of the BMZ decomposition, which mixes quasiparticle states, is equal to unity. Physically, it means that BCS approach cannot describe processes due to the quasi-

particle scattering. Therefore the phenomena which involve interaction of quasiparticles with nonuniform pairing field are out of range for the BCS approach. Hence, *e.g.*, such phenomena, related to the nonuniformity of the pairing field, as the existence of Andreev states or Andreev reflection, which are well-known in the condensed matter physics (also in the context of Josephson junction) cannot be described within the BCS framework. Since in the HF+BCS approach one finds occupation numbers of the HF orbitals, which are just numbers associated with each orbital, therefore it cannot describe a configuration with position dependent phase of the pairing field. For example, the stationary vortex solution cannot be obtained as it requires the occupation numbers to vary when one is approaching the core of the vortex where the system becomes normal (pairing field tends to zero). In other words, the BCS treatment introduces only one additional degree of freedom, which is related to the magnitude of the complex pairing field, but is unable to describe properly its excitation modes, *e.g.*, Bogoliubov phonons.

The situation in the case of TDHF+BCS approach is similar. The evolution is performed through the equations:

$$i\hbar \frac{\partial}{\partial t} \psi_k(\mathbf{r}, t) = \hat{h} \psi_k(\mathbf{r}, t), \quad (19)$$

which define the evolution of HF orbitals according to the mean-field  $\hat{h}$ , and  $|k\rangle = |\mathbf{k}\sigma\rangle$ . In addition, the equations describing the evolution of diagonal density matrix  $\rho$  and pairing tensor  $\nu$  in this basis are solved (see Refs. [10, 11]):

$$\frac{d}{dt} \rho_{kk} = \Delta_{k\bar{k}} \nu_{k\bar{k}}^* - \Delta_{k\bar{k}}^* \nu_{k\bar{k}}, \quad (20)$$

$$\frac{d}{dt} \nu_{k\bar{k}} = \Delta_{k\bar{k}} (1 - 2\rho_{kk}), \quad (21)$$

where  $\bar{k}$  is the time-reversal partner of the state  $k$ . These equations describe simply the evolution of the occupation numbers  $v_k$  and  $u_k$  of the HF orbitals because:

$$\rho(\mathbf{r}, t) = \sum_k |v_k(t)|^2 |\psi_k(\mathbf{r}, t)|^2, \quad (22)$$

$$\nu(\mathbf{r}, t) = \sum_k u_k(t) v_k(t) \psi_k(\mathbf{r}, t) \psi_{\bar{k}}(\mathbf{r}, t). \quad (23)$$

The spatial dependence of these occupation numbers is not included and consequently the dynamics of the pairing field is realized only through changes of the HF orbitals.

In order to give a simple example of the case where the TDHF+BCS method fails completely, let us imagine that we have a uniform system with a non-vanishing pairing gap. In such a case, the static HF+BCS treatment is equivalent to the HFB treatment, as there is no quasiparticle scattering in the system and the canonical basis



corresponds simply to plane waves. Now imagine that we apply an external, spatially modulated, pairing field  $\Delta_{\text{ext}}(\mathbf{r})$ . How the system will react? In the TDHF+BCS treatment this spatial modulation cannot be described, as the system of equations is initially in the canonical basis which corresponds to plane waves and these plane waves are eigenstates of the mean field:

$$\hat{h}\psi_k(\mathbf{r}, t) = \varepsilon_k\psi_k(\mathbf{r}, t). \quad (24)$$

Therefore HF orbitals will not change (apart from the phase change) and they will not be affected by the external pairing field. The modification of the above equations after the application of the external pairing field results in modifying the term:

$$\Delta_{k\bar{k}} \rightarrow \Delta_{k\bar{k}} + \Delta_{k\bar{k}}^{\text{ext}}. \quad (25)$$

Clearly,  $\Delta_{\text{ext}}(\mathbf{r})$  potential enters into the above equations in the form of the matrix element in the plane wave basis:  $\Delta_{k\bar{k}}^{\text{ext}} \propto \int \Delta_{\text{ext}}(\mathbf{r})d\mathbf{r}$ . Therefore it will only change the magnitude of the pairing field on average and will result in an average oscillations of the uniform pairing field. Since the density in this treatment is expressed by Eq. (22) and  $\psi_k \propto e^{i\mathbf{k}\cdot\mathbf{r}}$ , there is no mechanism to break the translational symmetry induced by the external pairing field as it only may occur through the symmetry breaking terms in the mean-field Hamiltonian (these are absent according to our initial assumption). This simple example clearly shows that in the TDHF+BCS treatment the degrees of freedom associated with the Cooper-pair dynamics are treated only in a very limited way and the pairing field dynamics is practically absent. The spatial modulation of the pairing field in the TDHF+BCS dynamics may occur only as a consequence of the evolution of the normal density  $\rho$ .

In the TDHFB treatment, on the other hand, the situation is radically different and the pairing field  $\Delta(\mathbf{r}, t)$  has its own degrees freedom treated on the same footing as the normal degrees of freedom described by  $\rho(\mathbf{r}, t)$ . They are of course coupled but formally independent. Consequently, in the TDHFB evolution, the modulation of the external pairing field will propagate leading to a variety of effects, including translational symmetry breaking of the mean-field, and giving rise to various quasiparticle scattering processes. These processes are beyond the simplified TDHF+BCS treatment. Last but not least, one has to keep in mind that TDHF+BCS equations violate the continuity equation which produce various unwanted effects (see Ref. [10]).

In summary, the effect studied in the paper is exactly of the nature that prevents its description by the TDHF+BCS approach. Namely, the excitation of the pairing modes in the form of a soliton induces also the modification of the normal density, however the dynamics is triggered by the dynamics of the pairing field which is induced by the spatial variation of the pairing field and cannot be described by the TDHF+BCS approach.

## MOVIES

### Central collisions of $^{240}\text{Pu} + ^{240}\text{Pu}$

The movies show sections along the reaction plane. Each movie displays 10 panels organized in a grid of 2 columns and 5 rows. The left column presents the total density (density of protons + density of neutrons), while the right column presents absolute value of the pairing field of neutrons. In each row dynamics of the system for pairing phase difference  $\Delta\varphi$  is shown. The phase differences are from 0 (bottom row) to  $\pi$  (top row) with an increment  $\pi/4$ . The only difference in initial states is the phase difference, all other quantities (like energy, density distribution, etc.) are exactly the same (up to machine precision). Thus, all differences in the dynamics are due to the pairing effects. Below we provide 8 movies for different collision energies from a range  $E \in [1.04 V_{\text{Bass}}, 1.50 V_{\text{Bass}}]$ , where  $V_{\text{Bass}} = 897.31$  MeV is the phenomenological fusion barrier [6]. The value of the collision energy is encoded in the file name.

1. File: 240Pu+240Pu\_1.04V.mp4  
YouTube: <https://youtu.be/foA33kCPT5g>
2. File: 240Pu+240Pu\_1.07V.mp4  
YouTube: <https://youtu.be/jiWpUUAe7Uw>
3. File: 240Pu+240Pu\_1.09V.mp4  
YouTube: <https://youtu.be/0YiBJ1PFVnA>
4. File: 240Pu+240Pu\_1.15V.mp4  
YouTube: <https://youtu.be/It1ZQRw9yDs>
5. File: 240Pu+240Pu\_1.20V.mp4  
YouTube: <https://youtu.be/bXTzRW2HgTQ>
6. File: 240Pu+240Pu\_1.30V.mp4  
YouTube: <https://youtu.be/7UstUB6DBn4>
7. File: 240Pu+240Pu\_1.40V.mp4  
YouTube: <https://youtu.be/rHLSWPYj798>
8. File: 240Pu+240Pu\_1.50V.mp4  
YouTube: <https://youtu.be/YH0wSPoU5ag>

### Central collisions of $^{90}\text{Zr} + ^{90}\text{Zr}$

The movies are analogues to the movies for  $^{240}\text{Pu} + ^{240}\text{Pu}$  collisions. For some energies not all panels are filled with data. These are situations that correspond to the fusion process. Moreover, for some cases one can notice that the system slowly rotates after collision. The effect originates from the fact that the collisions are not perfectly central (due to small numerical noise). Below we provide 12 movies for different collision energies from a range  $E \in [0.98 V_{\text{Bass}}, 1.15 V_{\text{Bass}}]$ , where



$V_{\text{Bass}} = 192.47$  MeV and the value of the collision energy is encoded in the file name.

1. File: 90Zr+90Zr\_0.98V.mp4  
YouTube: <https://youtu.be/YcATJ6pMgD0>
2. File: 90Zr+90Zr\_0.99V.mp4  
YouTube: <https://youtu.be/amXMsxw1Wd0>
3. File: 90Zr+90Zr\_1.00V.mp4  
YouTube: <https://youtu.be/zE74gdLTgWw>
4. File: 90Zr+90Zr\_1.02V.mp4  
YouTube: <https://youtu.be/UEPiwEZDeYc>
5. File: 90Zr+90Zr\_1.03V.mp4  
YouTube: <https://youtu.be/Ubs3g12UW5U>
6. File: 90Zr+90Zr\_1.04V.mp4  
YouTube: <https://youtu.be/GysuioTC7mY>
7. File: 90Zr+90Zr\_1.05V.mp4  
YouTube: <https://youtu.be/cNbiadr7i48>
8. File: 90Zr+90Zr\_1.11V.mp4  
YouTube: <https://youtu.be/7Rc70bbnkx8>
9. File: 90Zr+90Zr\_1.12V.mp4  
YouTube: [https://youtu.be/CZ\\_d19vIbtI](https://youtu.be/CZ_d19vIbtI)
10. File: 90Zr+90Zr\_1.13V.mp4  
YouTube: <https://youtu.be/jv5iyFFrqBI>
11. File: 90Zr+90Zr\_1.14V.mp4  
YouTube: <https://youtu.be/sPH9PNEIVo4>
12. File: 90Zr+90Zr\_1.15V.mp4  
YouTube: [https://youtu.be/U3t\\_xcdrWTA](https://youtu.be/U3t_xcdrWTA)

#### Non-central collisions of $^{90}\text{Zr} + ^{90}\text{Zr}$

We also provide 3 movies demonstrating the impact of the phase difference on dynamics of non-central collisions. For better visibility we display only results for 3 phase differences: 0 (bottom row),  $\frac{\pi}{2}$  (middle row) and  $\pi$  (top

row). The collisions are for fixed collision energy and 3 different impact parameters.

1. File: 90Zr+90Zr\_noncentral11\_1.38V.mp4  
YouTube: <https://youtu.be/bOLhIEmfFSQ>
2. File: 90Zr+90Zr\_noncentral12\_1.38V.mp4  
YouTube: <https://youtu.be/N72VQJVo4aI>
3. File: 90Zr+90Zr\_noncentral13\_1.38V.mp4  
YouTube: <https://youtu.be/UCCAN9ahNqA>

- 
- \* Electronic address: magiersk@if.pw.edu.pl, sekizawa@if.pw.edu.pl, gabrielw@if.pw.edu.pl
- [1] G. Wlazlowski, K. Sekizawa, P. Magierski, A. Bulgac, and M.M. Forbes, Vortex Pinning and Dynamics in the Neutron Star Crust, *Phys. Rev. Lett.* **117**, 232701 (2016).
  - [2] Yongle Yu and Aurel Bulgac, Energy Density Functional Approach to Superfluid Nuclei, *Phys. Rev. Lett.* **90**, 222501 (2003).
  - [3] A. Bulgac and Y. Yu, Renormalization of the Hartree-Fock-Bogoliubov Equations in the Case of a Zero Range Pairing Interaction, *Phys. Rev. Lett.* **88**, 042504 (2002).
  - [4] A. Bulgac, Local Density Approximation for Systems with Pairing Correlations, *Phys. Rev. C* **65** 051305(R) (2002).
  - [5] S. Jin, A. Bulgac, K. Roche, and G. Wlazlowski, Coordinate-Space Solver for Superfluid Many-Fermion Systems with Shifted Conjugate Orthogonal Conjugate Gradient Method, *Phys. Rev. C* **95**, 044302 (2017).
  - [6] R. Bass, Fusion of heavy nuclei in a classical model, *Nucl. Phys.* **A231**, 45 (1974).
  - [7] C. Golabek and C. Simenel, Collision dynamics of two  $^{238}\text{U}$  atomic nuclei, *Phys. Rev. Lett.* **103**, 042701 (2009).
  - [8] C. Bloch and A. Messiah, The canonical form of an antisymmetric tensor and its application to the theory of superconductivity, *Nucl. Phys.* **39**, 95 (1962).
  - [9] B. Zumino, Normal Forms of Complex Matrices, *J. Math. Phys.* **3**, 1055 (1962).
  - [10] G. Scamps, D. Lacroix, G.F. Bertsch, and K. Washiyama, Pairing dynamics in particle transport, *Phys. Rev. C* **85**, 034328 (2012).
  - [11] S. Ebata, T. Nakatsukasa, T. Inakura, K. Yoshida, Y. Hashimoto, and K. Yabana, Canonical-basis time-dependent Hartree-Fock-Bogoliubov theory and linear-response calculations, *Phys. Rev. C* **82**, 034306 (2010).